Precision Measurement of Cosmic-Ray Nitrogen and its Primary and Secondary Components with the Alpha Magnetic Spectrometer on the International Space Station
- SUPPLEMENTAL MATERIAL -

(AMS Collaboration)

For references see the main text.

Detector.— The tracker has nine layers, the first $L1$ at the top of the detector, the second $L2$ above the magnet, six $L3$ to $L8$ within the bore of the magnet, and the last $L9$ above the ECAL. $L2$ to $L8$ constitute the inner tracker. Each layer of the tracker provides an independent measurement of the charge Z with a resolution of $\Delta Z/Z = 4.5\%$ for nitrogen, where ΔZ is the root mean square (rms) width of the Z distribution. Overall, the inner tracker has a resolution of $\Delta Z/Z = 1.7\%$. The spatial resolution in each tracker layer is 5.5 μm for nitrogen in the bending direction. Together, the tracker and the magnet measure the rigidity R of nitrogen nuclei with a maximum detectable rigidity (MDR) of 3.5 TV over the 3 m lever arm from $L1$ to $L9$.

Two of the TOF planes are located above the magnet (upper TOF) and two planes are below the magnet (lower TOF). The overall velocity ($\beta = v/c$) resolution has been measured to be $\Delta\beta/\beta^2 = 0.01$ for $Z = 7$ nuclei. This discriminates between upward- and downward-going particles. The pulse heights of the two upper planes are combined to provide an independent measurement of the charge with an accuracy $\Delta Z/Z = 2\%$. The pulse heights from the two lower planes are combined to provide another independent charge measurement with the same accuracy.

Data Analysis.— To verify the MC predictions, the fraction of nitrogen events that traverse materials between $L8$ and $L9$ (lower TOF and RICH) without interacting were measured in data and compared with simulations with the inelastic cross sections varied within $\pm 10\%$. The resulting cross sections with the best agreement to data were chosen. Figure SM 5 shows the good agreement between the measured nitrogen nuclei survival probability from $L8$ to $L9$ compared with the simulation, where the survival probability is defined as the ratio of events which have the same charge value measured by $L1$–$L9$ to events which have the same charge value measured by $L1$–$L8$. Similarly, the survival probabilities between $L1$ and $L2$ have been calculated using data collected when AMS was horizontal, i.e.$\sim 90^\circ$ with respect to the zenith [18]. This independently verifies the inelastic cross sections. The systematic error on the flux due to the uncertainties of inelastic cross sections is evaluated to be $<3\%$ up to 100 GV. At higher rigidities, the small rigidity dependencies of the cross sections from the Glauber-Gribov model were treated as an uncertainty and added in quadrature to the uncertainties from the measured interaction probabilities. Combining all sources, the resulting systematic errors on the flux associated with the acceptance were evaluated to be 4% at 3.3 TV.

TABLE SM I: The nitrogen flux Φ_N as a function of rigidity at the top of AMS in units of $[m^2 \cdot sr \cdot s \cdot GV]^{-1}$ including errors due to statistics (stat.); contributions to the systematic error from the trigger, acceptance and background contamination (acc.); the rigidity resolution function and unfolding (unf.); and the total systematic error (syst.). The contribution of individual sources to the systematic error are added in quadrature to arrive at the total systematic error. The Monte Carlo event samples have sufficient statistics such that they do not contribute to the errors.

Rigidity [GV]	Φ_N	$\sigma_{stat.}$	$\sigma_{acc.}$	$\sigma_{unf.}$	σ_{scale}	$\sigma_{syst.}$	
2.15 – 2.40	(3.825	0.018	0.124	0.047	0.016	0.133)	$\times 10^{-1}$
2.40 – 2.67	(3.757	0.016	0.120	0.033	0.009	0.124)	$\times 10^{-1}$
2.67 – 2.97	(3.491	0.014	0.110	0.027	0.005	0.113)	$\times 10^{-1}$
2.97 – 3.29	(3.166	0.012	0.099	0.021	0.002	0.101)	$\times 10^{-1}$
3.29 – 3.64	(2.822	0.010	0.088	0.017	0.000	0.089)	$\times 10^{-1}$
3.64 – 4.02	(2.441	0.009	0.076	0.013	0.001	0.077)	$\times 10^{-1}$
4.02 – 4.43	(2.106	0.007	0.065	0.010	0.002	0.066)	$\times 10^{-1}$
4.43 – 4.88	(1.792	0.006	0.055	0.008	0.003	0.056)	$\times 10^{-1}$
4.88 – 5.37	(1.508	0.005	0.047	0.006	0.003	0.047)	$\times 10^{-1}$
5.37 – 5.90	(1.260	0.004	0.039	0.004	0.003	0.039)	$\times 10^{-1}$
5.90 – 6.47	(1.035	0.003	0.032	0.003	0.002	0.032)	$\times 10^{-1}$
6.47 – 7.09	(8.589	0.028	0.266	0.025	0.022	0.268)	$\times 10^{-2}$
7.09 – 7.76	(6.981	0.023	0.217	0.020	0.019	0.218)	$\times 10^{-2}$
7.76 – 8.48	(5.711	0.019	0.177	0.015	0.017	0.179)	$\times 10^{-2}$
8.48 – 9.26	(4.653	0.016	0.145	0.012	0.015	0.146)	$\times 10^{-2}$
9.26 – 10.1	(3.774	0.013	0.118	0.009	0.012	0.119)	$\times 10^{-2}$
10.1 – 11.0	(3.047	0.011	0.095	0.007	0.010	0.096)	$\times 10^{-2}$
11.0 – 12.0	(2.471	0.010	0.077	0.006	0.009	0.078)	$\times 10^{-2}$
12.0 – 13.0	(1.988	0.008	0.062	0.005	0.007	0.063)	$\times 10^{-2}$
13.0 – 14.1	(1.624	0.007	0.051	0.004	0.006	0.051)	$\times 10^{-2}$
14.1 – 15.3	(1.326	0.006	0.042	0.003	0.005	0.042)	$\times 10^{-2}$
15.3 – 16.6	(1.072	0.005	0.034	0.003	0.004	0.034)	$\times 10^{-2}$
16.6 – 18.0	(8.688	0.044	0.273	0.022	0.035	0.276)	$\times 10^{-3}$
18.0 – 19.5	(6.966	0.037	0.220	0.018	0.028	0.222)	$\times 10^{-3}$
19.5 – 21.1	(5.659	0.031	0.179	0.016	0.023	0.181)	$\times 10^{-3}$
21.1 – 22.8	(4.627	0.026	0.146	0.013	0.019	0.148)	$\times 10^{-3}$
22.8 – 24.7	(3.670	0.021	0.116	0.011	0.016	0.118)	$\times 10^{-3}$
24.7 – 26.7	(2.959	0.018	0.094	0.009	0.013	0.095)	$\times 10^{-3}$
26.7 – 28.8	(2.380	0.015	0.076	0.008	0.010	0.077)	$\times 10^{-3}$
28.8 – 31.1	(1.940	0.013	0.062	0.007	0.009	0.063)	$\times 10^{-3}$
31.1 – 33.5	(1.550	0.011	0.050	0.006	0.007	0.051)	$\times 10^{-3}$
33.5 – 36.1	(1.260	0.009	0.041	0.005	0.006	0.041)	$\times 10^{-3}$
36.1 – 38.9	(1.021	0.008	0.033	0.004	0.005	0.034)	$\times 10^{-3}$
38.9 – 41.9	(8.116	0.069	0.263	0.034	0.039	0.268)	$\times 10^{-4}$
41.9 – 45.1	(6.701	0.061	0.217	0.030	0.032	0.222)	$\times 10^{-4}$
45.1 – 48.5	(5.461	0.053	0.178	0.025	0.027	0.181)	$\times 10^{-4}$
48.5 – 52.2	(4.479	0.046	0.146	0.022	0.022	0.150)	$\times 10^{-4}$

Table continued

TABLE SM I – *(Continued).*

Rigidity [GV]	$\Phi_{\rm N}$	$\sigma_{\rm stat.}$	$\sigma_{\rm acc.}$	$\sigma_{\rm unf.}$	$\sigma_{\rm scale}$	$\sigma_{\rm syst.}$	
52.2 – 56.1	(3.473	0.039	0.114	0.018	0.018	0.117)	$\times 10^{-4}$
56.1 – 60.3	(2.819	0.034	0.093	0.015	0.015	0.095)	$\times 10^{-4}$
60.3 – 64.8	(2.349	0.030	0.078	0.013	0.012	0.080)	$\times 10^{-4}$
64.8 – 69.7	(1.883	0.026	0.063	0.011	0.010	0.064)	$\times 10^{-4}$
69.7 – 74.9	(1.484	0.022	0.050	0.009	0.008	0.051)	$\times 10^{-4}$
74.9 – 80.5	(1.236	0.020	0.041	0.008	0.007	0.043)	$\times 10^{-4}$
80.5 – 86.5	(1.007	0.017	0.034	0.007	0.006	0.035)	$\times 10^{-4}$
86.5 – 93.0	(8.182	0.148	0.276	0.059	0.049	0.286)	$\times 10^{-5}$
93.0 – 100	(6.503	0.127	0.220	0.049	0.040	0.229)	$\times 10^{-5}$
100 – 108	(5.385	0.108	0.183	0.043	0.034	0.191)	$\times 10^{-5}$
108 – 116	(4.071	0.094	0.140	0.034	0.026	0.146)	$\times 10^{-5}$
116 – 125	(3.399	0.081	0.117	0.030	0.023	0.123)	$\times 10^{-5}$
125 – 135	(2.743	0.069	0.095	0.025	0.019	0.100)	$\times 10^{-5}$
135 – 147	(2.182	0.056	0.076	0.021	0.016	0.080)	$\times 10^{-5}$
147 – 160	(1.675	0.047	0.058	0.017	0.013	0.062)	$\times 10^{-5}$
160 – 175	(1.323	0.039	0.046	0.014	0.010	0.049)	$\times 10^{-5}$
175 – 192	(1.010	0.032	0.036	0.011	0.008	0.038)	$\times 10^{-5}$
192 – 211	(7.264	0.256	0.260	0.088	0.064	0.282)	$\times 10^{-6}$
211 – 233	(6.068	0.218	0.214	0.078	0.058	0.235)	$\times 10^{-6}$
233 – 259	(4.400	0.170	0.157	0.061	0.045	0.174)	$\times 10^{-6}$
259 – 291	(3.352	0.134	0.119	0.051	0.038	0.135)	$\times 10^{-6}$
291 – 330	(2.378	0.102	0.085	0.039	0.030	0.098)	$\times 10^{-6}$
330 – 379	(1.706	0.077	0.061	0.031	0.024	0.073)	$\times 10^{-6}$
379 – 441	(1.061	0.054	0.039	0.022	0.017	0.048)	$\times 10^{-6}$
441 – 525	(6.952	0.377	0.254	0.165	0.134	0.331)	$\times 10^{-7}$
525 – 660	(3.943	0.224	0.145	0.112	0.093	0.206)	$\times 10^{-7}$
660 – 880	(2.160	0.130	0.080	0.079	0.065	0.130)	$\times 10^{-7}$
880 – 1300	(9.327	0.621	0.356	0.469	0.376	0.699)	$\times 10^{-8}$
1300 – 3300	(1.646	0.287	0.074	0.049	0.079	0.119)	$\times 10^{-8}$

TABLE SM II: The nitrogen to oxygen flux ratio N/O as a function of rigidity including errors due to statistics (stat.); contributions to the systematic error from the trigger, acceptance and background contamination (acc.); the rigidity resolution function and unfolding (unf.); the absolute rigidity scale (scale); and the total systematic error (syst.). The statistical errors are the quadratic sum of the relative statistical errors of the nitrogen and oxygen fluxes multiplied by the N/O ratio. The systematic errors from the background subtraction, the trigger, and the event reconstruction and selection are likewise added in quadrature. The correlations in the systematic errors from the uncertainty in nuclear interaction cross sections, the unfolding and the absolute rigidity scale between the nitrogen and oxygen fluxes have been taken into account in calculating the corresponding systematic errors of the N/O ratio. The contribution of individual sources to the systematic error are added in quadrature to arrive at the total systematic uncertainty. Note that we have recomputed the oxygen flux above 525 GV to the bins used for nitrogen.

Rigidity [GV]	N/O	$\sigma_{\text{stat.}}$	$\sigma_{\text{acc.}}$	$\sigma_{\text{unf.}}$	σ_{scale}	$\sigma_{\text{syst.}}$
2.15 – 2.40	0.2762	0.0015	0.0071	0.0034	0.0002	0.0079
2.40 – 2.67	0.2901	0.0014	0.0070	0.0028	0.0002	0.0076
2.67 – 2.97	0.2946	0.0013	0.0068	0.0024	0.0001	0.0073
2.97 – 3.29	0.2973	0.0013	0.0067	0.0021	0.0000	0.0070
3.29 – 3.64	0.3013	0.0012	0.0066	0.0018	0.0000	0.0069
3.64 – 4.02	0.2996	0.0012	0.0065	0.0016	0.0000	0.0067
4.02 – 4.43	0.3007	0.0012	0.0064	0.0014	0.0000	0.0066
4.43 – 4.88	0.2992	0.0011	0.0063	0.0012	0.0000	0.0065
4.88 – 5.37	0.2972	0.0011	0.0063	0.0011	0.0000	0.0064
5.37 – 5.90	0.2953	0.0011	0.0062	0.0010	0.0001	0.0063
5.90 – 6.47	0.2899	0.0011	0.0061	0.0009	0.0001	0.0062
6.47 – 7.09	0.2895	0.0011	0.0061	0.0008	0.0001	0.0062
7.09 – 7.76	0.2848	0.0011	0.0061	0.0007	0.0001	0.0061
7.76 – 8.48	0.2811	0.0011	0.0060	0.0007	0.0001	0.0061
8.48 – 9.26	0.2775	0.0011	0.0060	0.0006	0.0001	0.0060
9.26 – 10.1	0.2735	0.0011	0.0059	0.0006	0.0001	0.0059
10.1 – 11.0	0.2693	0.0011	0.0058	0.0006	0.0001	0.0059
11.0 – 12.0	0.2661	0.0012	0.0058	0.0006	0.0001	0.0058
12.0 – 13.0	0.2592	0.0012	0.0057	0.0006	0.0001	0.0057
13.0 – 14.1	0.2563	0.0013	0.0056	0.0006	0.0001	0.0057
14.1 – 15.3	0.2560	0.0013	0.0057	0.0006	0.0001	0.0057
15.3 – 16.6	0.2501	0.0014	0.0056	0.0006	0.0001	0.0056
16.6 – 18.0	0.2470	0.0014	0.0055	0.0006	0.0001	0.0056
18.0 – 19.5	0.2405	0.0014	0.0054	0.0006	0.0001	0.0054
19.5 – 21.1	0.2377	0.0015	0.0054	0.0006	0.0001	0.0054
21.1 – 22.8	0.2367	0.0015	0.0054	0.0006	0.0001	0.0054
22.8 – 24.7	0.2275	0.0015	0.0052	0.0006	0.0001	0.0053
24.7 – 26.7	0.2244	0.0015	0.0052	0.0007	0.0001	0.0052
26.7 – 28.8	0.2201	0.0015	0.0051	0.0007	0.0001	0.0052
28.8 – 31.1	0.2173	0.0016	0.0051	0.0007	0.0001	0.0051
31.1 – 33.5	0.2104	0.0016	0.0050	0.0007	0.0001	0.0050

Table continued

TABLE SM II – *(Continued).*

Rigidity [GV]	N/O	$\sigma_{\text{stat.}}$	$\sigma_{\text{acc.}}$	$\sigma_{\text{unf.}}$	σ_{scale}	$\sigma_{\text{syst.}}$
33.5 – 36.1	0.2076	0.0017	0.0050	0.0008	0.0001	0.0050
36.1 – 38.9	0.2045	0.0018	0.0049	0.0008	0.0002	0.0050
38.9 – 41.9	0.1989	0.0019	0.0048	0.0008	0.0002	0.0049
41.9 – 45.1	0.1986	0.0020	0.0049	0.0008	0.0002	0.0049
45.1 – 48.5	0.1962	0.0021	0.0049	0.0009	0.0002	0.0049
48.5 – 52.2	0.1935	0.0022	0.0048	0.0009	0.0002	0.0049
52.2 – 56.1	0.1820	0.0023	0.0046	0.0009	0.0002	0.0047
56.1 – 60.3	0.1810	0.0024	0.0047	0.0009	0.0002	0.0047
60.3 – 64.8	0.1821	0.0026	0.0047	0.0010	0.0002	0.0048
64.8 – 69.7	0.1770	0.0027	0.0047	0.0010	0.0002	0.0048
69.7 – 74.9	0.1723	0.0028	0.0046	0.0010	0.0002	0.0047
74.9 – 80.5	0.1726	0.0030	0.0046	0.0010	0.0002	0.0048
80.5 – 86.5	0.1698	0.0031	0.0046	0.0011	0.0002	0.0047
86.5 – 93.0	0.1697	0.0033	0.0047	0.0011	0.0002	0.0048
93.0 – 100	0.1650	0.0035	0.0046	0.0011	0.0002	0.0047
100 – 108	0.1661	0.0036	0.0047	0.0012	0.0002	0.0048
108 – 116	0.1521	0.0038	0.0044	0.0011	0.0002	0.0045
116 – 125	0.1558	0.0040	0.0045	0.0012	0.0002	0.0047
125 – 135	0.1540	0.0042	0.0045	0.0012	0.0002	0.0047
135 – 147	0.1505	0.0042	0.0045	0.0013	0.0002	0.0047
147 – 160	0.1494	0.0045	0.0045	0.0013	0.0002	0.0047
160 – 175	0.1486	0.0047	0.0045	0.0014	0.0002	0.0047
175 – 192	0.1435	0.0049	0.0045	0.0014	0.0002	0.0047
192 – 211	0.1302	0.0049	0.0042	0.0014	0.0002	0.0044
211 – 233	0.1448	0.0056	0.0046	0.0016	0.0002	0.0049
233 – 259	0.1388	0.0058	0.0045	0.0017	0.0002	0.0048
259 – 291	0.1414	0.0061	0.0046	0.0019	0.0002	0.0050
291 – 330	0.1395	0.0064	0.0047	0.0020	0.0002	0.0051
330 – 379	0.1396	0.0068	0.0047	0.0022	0.0002	0.0052
379 – 441	0.1291	0.0070	0.0045	0.0023	0.0002	0.0051
441 – 525	0.1323	0.0077	0.0047	0.0028	0.0002	0.0055
525 – 660	0.1315	0.0080	0.0048	0.0033	0.0001	0.0058
660 – 880	0.1382	0.0089	0.0052	0.0046	0.0000	0.0069
880 – 1300	0.1382	0.0099	0.0054	0.0064	0.0002	0.0083
1300 – 3300	0.1225	0.0227	0.0060	0.0042	0.0003	0.0074

TABLE SM III: The nitrogen to boron flux ratio N/B as a function of rigidity including errors due to statistics (stat.); contributions to the systematic error from the trigger, acceptance and background contamination (acc.); the rigidity resolution function and unfolding (unf.); the absolute rigidity scale (scale); and the total systematic error (syst.). The statistical errors are the quadratic sum of the relative statistical errors of the nitrogen and boron fluxes multiplied by the N/B ratio. The systematic errors from the background subtraction, the trigger, and the event reconstruction and selection are likewise added in quadrature. The correlations in the systematic errors from the uncertainty in nuclear interaction cross sections, the unfolding and the absolute rigidity scale between the nitrogen and boron fluxes have been taken into account in calculating the corresponding systematic errors of the N/B ratio. The contribution of individual sources to the systematic error are added in quadrature to arrive at the total systematic uncertainty.

Rigidity [GV]	N/B	$\sigma_{\text{stat.}}$	$\sigma_{\text{acc.}}$	$\sigma_{\text{unf.}}$	σ_{scale}	$\sigma_{\text{syst.}}$
2.15 – 2.40	0.8992	0.0057	0.0440	0.0100	0.0003	0.0451
2.40 – 2.67	0.8897	0.0051	0.0393	0.0074	0.0001	0.0400
2.67 – 2.97	0.8870	0.0047	0.0357	0.0064	0.0002	0.0363
2.97 – 3.29	0.8869	0.0045	0.0328	0.0056	0.0002	0.0332
3.29 – 3.64	0.8863	0.0042	0.0303	0.0049	0.0001	0.0307
3.64 – 4.02	0.8734	0.0041	0.0279	0.0042	0.0000	0.0282
4.02 – 4.43	0.8735	0.0040	0.0263	0.0038	0.0001	0.0266
4.43 – 4.88	0.8850	0.0039	0.0254	0.0034	0.0002	0.0256
4.88 – 5.37	0.8793	0.0037	0.0242	0.0031	0.0002	0.0244
5.37 – 5.90	0.8895	0.0038	0.0237	0.0029	0.0003	0.0238
5.90 – 6.47	0.8885	0.0038	0.0230	0.0027	0.0003	0.0232
6.47 – 7.09	0.9014	0.0039	0.0229	0.0027	0.0003	0.0231
7.09 – 7.76	0.9054	0.0040	0.0227	0.0026	0.0003	0.0228
7.76 – 8.48	0.9152	0.0041	0.0226	0.0026	0.0003	0.0228
8.48 – 9.26	0.9219	0.0042	0.0226	0.0026	0.0002	0.0227
9.26 – 10.1	0.9302	0.0044	0.0227	0.0026	0.0002	0.0228
10.1 – 11.0	0.9282	0.0047	0.0225	0.0026	0.0002	0.0226
11.0 – 12.0	0.9481	0.0050	0.0229	0.0026	0.0003	0.0231
12.0 – 13.0	0.9443	0.0054	0.0228	0.0026	0.0003	0.0229
13.0 – 14.1	0.9619	0.0058	0.0232	0.0026	0.0003	0.0234
14.1 – 15.3	0.9781	0.0062	0.0236	0.0026	0.0003	0.0238
15.3 – 16.6	0.9826	0.0065	0.0238	0.0026	0.0004	0.0239
16.6 – 18.0	1.0107	0.0071	0.0246	0.0027	0.0004	0.0247
18.0 – 19.5	0.9987	0.0073	0.0244	0.0027	0.0004	0.0245
19.5 – 21.1	1.0221	0.0078	0.0251	0.0028	0.0004	0.0252
21.1 – 22.8	1.0497	0.0082	0.0259	0.0029	0.0005	0.0261
22.8 – 24.7	1.0445	0.0083	0.0260	0.0029	0.0005	0.0262
24.7 – 26.7	1.0524	0.0088	0.0263	0.0030	0.0005	0.0265
26.7 – 28.8	1.0481	0.0091	0.0264	0.0031	0.0005	0.0266
28.8 – 31.1	1.1005	0.0100	0.0280	0.0034	0.0005	0.0282
31.1 – 33.5	1.1034	0.0108	0.0284	0.0035	0.0006	0.0286
33.5 – 36.1	1.1051	0.0114	0.0287	0.0037	0.0006	0.0289

Table continued

TABLE SM III – *(Continued).*

Rigidity [GV]	N/B	$\sigma_{\text{stat.}}$	$\sigma_{\text{acc.}}$	$\sigma_{\text{unf.}}$	σ_{scale}	$\sigma_{\text{syst.}}$
36.1 – 38.9	1.1302	0.0125	0.0297	0.0040	0.0006	0.0299
38.9 – 41.9	1.1488	0.0138	0.0306	0.0042	0.0007	0.0309
41.9 – 45.1	1.1724	0.0151	0.0314	0.0045	0.0007	0.0318
45.1 – 48.5	1.1694	0.0162	0.0316	0.0048	0.0007	0.0319
48.5 – 52.2	1.2352	0.0183	0.0340	0.0053	0.0008	0.0345
52.2 – 56.1	1.1826	0.0192	0.0331	0.0053	0.0008	0.0335
56.1 – 60.3	1.2037	0.0209	0.0341	0.0057	0.0008	0.0346
60.3 – 64.8	1.2650	0.0236	0.0362	0.0063	0.0009	0.0368
64.8 – 69.7	1.2730	0.0254	0.0370	0.0067	0.0010	0.0376
69.7 – 74.9	1.2553	0.0273	0.0370	0.0069	0.0010	0.0377
74.9 – 80.5	1.2804	0.0296	0.0381	0.0075	0.0012	0.0388
80.5 – 86.5	1.3084	0.0325	0.0394	0.0080	0.0013	0.0403
86.5 – 93.0	1.2990	0.0343	0.0395	0.0084	0.0014	0.0404
93.0 – 100	1.3397	0.0385	0.0416	0.0091	0.0016	0.0426
100 – 108	1.4221	0.0427	0.0450	0.0103	0.0018	0.0462
108 – 116	1.3732	0.0469	0.0445	0.0105	0.0019	0.0458
116 – 125	1.3441	0.0471	0.0433	0.0109	0.0020	0.0447
125 – 135	1.4564	0.0551	0.0482	0.0126	0.0023	0.0498
135 – 147	1.4738	0.0572	0.0494	0.0137	0.0025	0.0513
147 – 160	1.5489	0.0668	0.0532	0.0155	0.0028	0.0555
160 – 175	1.5146	0.0679	0.0519	0.0164	0.0029	0.0545
175 – 192	1.4413	0.0685	0.0495	0.0170	0.0029	0.0524
192 – 211	1.4305	0.0756	0.0506	0.0185	0.0030	0.0540
211 – 233	1.5945	0.0883	0.0564	0.0227	0.0035	0.0609
233 – 259	1.5394	0.0911	0.0550	0.0244	0.0035	0.0602
259 – 291	1.8068	0.1157	0.0676	0.0320	0.0042	0.0749
291 – 330	1.6711	0.1123	0.0608	0.0335	0.0039	0.0695
330 – 379	1.9240	0.1420	0.0731	0.0441	0.0044	0.0855
379 – 441	1.7649	0.1429	0.0661	0.0470	0.0040	0.0812
441 – 525	1.7983	0.1555	0.0679	0.0567	0.0039	0.0886
525 – 660	1.7049	0.1521	0.0635	0.0666	0.0039	0.0921
660 – 880	2.1427	0.2176	0.0817	0.1104	0.0069	0.1375
880 – 1300	2.1107	0.2357	0.0794	0.1544	0.0128	0.1741
1300 – 3300	3.1220	1.0087	0.1648	0.2242	0.0461	0.2820

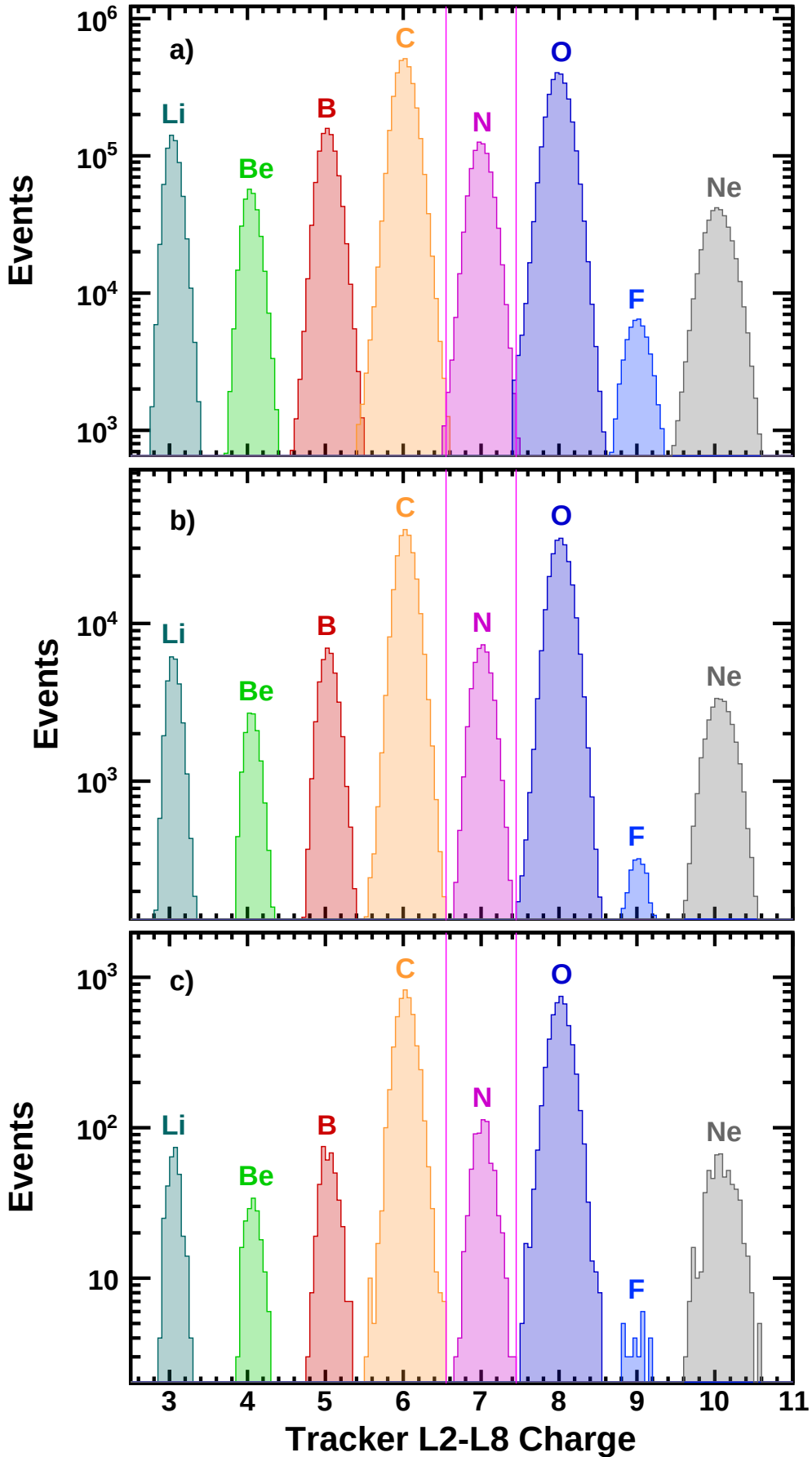

FIG. SM 1. Distribution of the charge measured with the inner tracker $L2$-$L8$ for samples from $Z = 3$ to $Z = 10$ selected by the combined charge measured with $L1$, the upper TOF, and the lower TOF with the rigidity ranges from (a) 4 GV to 38.9 GV, (b) 38.9 GV to 379 GV, and (c) 379 GV to 3300 GV. As seen, the tracker charge resolution $\Delta Z/Z$ does not depend on rigidity. The vertical lines correspond to the charge selection in the inner tracker for nitrogen. As seen, nitrogen events are well separated from carbon and oxygen at all rigidities.

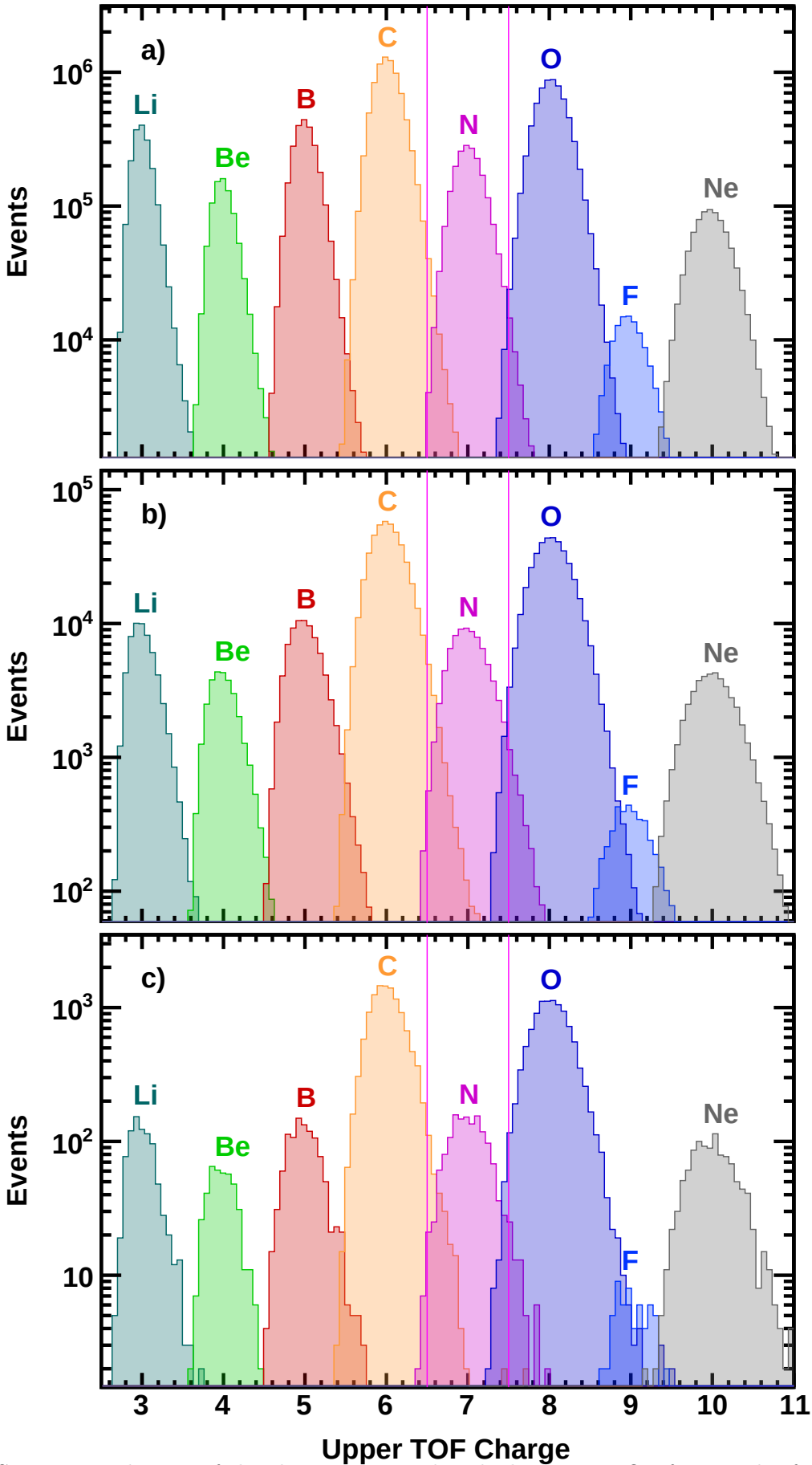

FIG. SM 2. Distribution of the charge measured with the upper TOF for samples from $Z = 3$ to $Z = 10$ selected by the combined charge measured with $L1$ and the inner tracker $L2$-$L8$ with the rigidity range from (a) 4 GV to 38.9 GV, (b) 38.9 GV to 379 GV and (c) 379 GV to 3300 GV. The vertical lines correspond to the charge selection in the upper TOF for nitrogen.

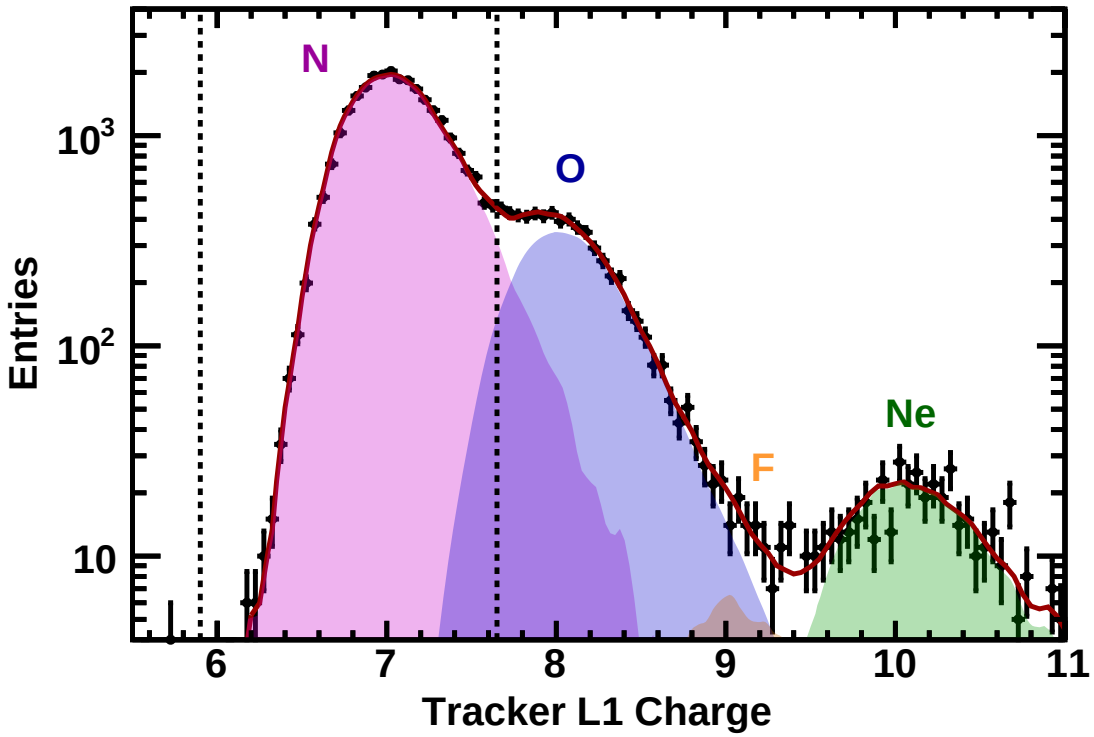

FIG. SM 3. The charge distributions measured by tracker $L1$ for nitrogen events selected by the inner tracker in the rigidity range between 9 and 11 GV (black dots). The solid red curve shows the fit to the data of the N, O, F, and Ne charge distribution templates. The templates are obtained from non-interacting samples at $L2$ by requiring the same change value at $L1$ and $L3$-$L8$. The charge selection cuts applied on tracker $L1$ are shown as vertical dashed lines.

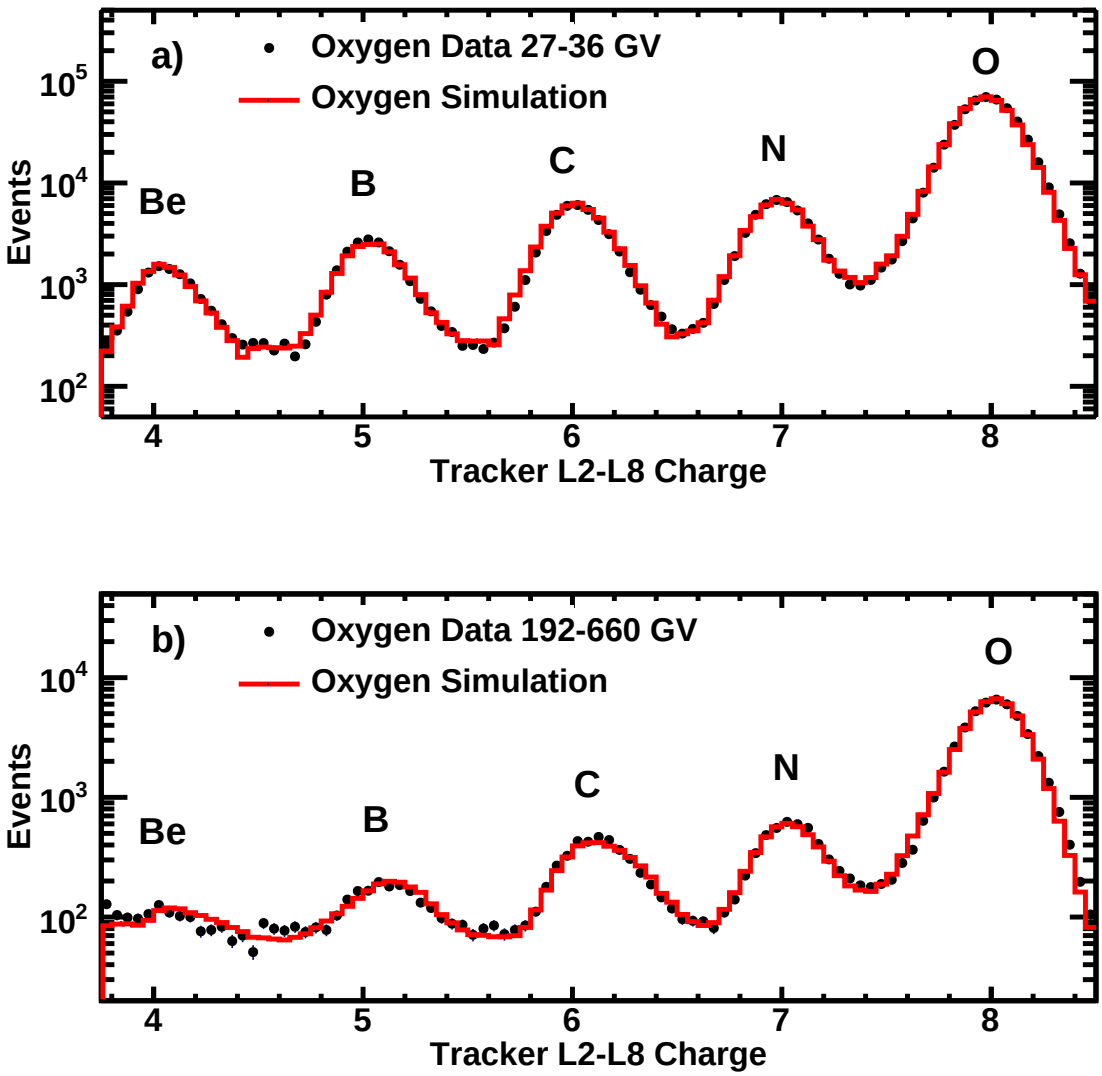

FIG. SM 4. The charge distribution measured by the inner tracker $L2$–$L8$, MDR $\sim$ 700 GV, for a sample of oxygen selected with tracker $L1$ in the rigidity ranges between (a) 27 and 36 GV and (b) 192 and 660 GV. MC distributions (histograms) are normalized to the non-interacting oxygen peak measured in the data (points).

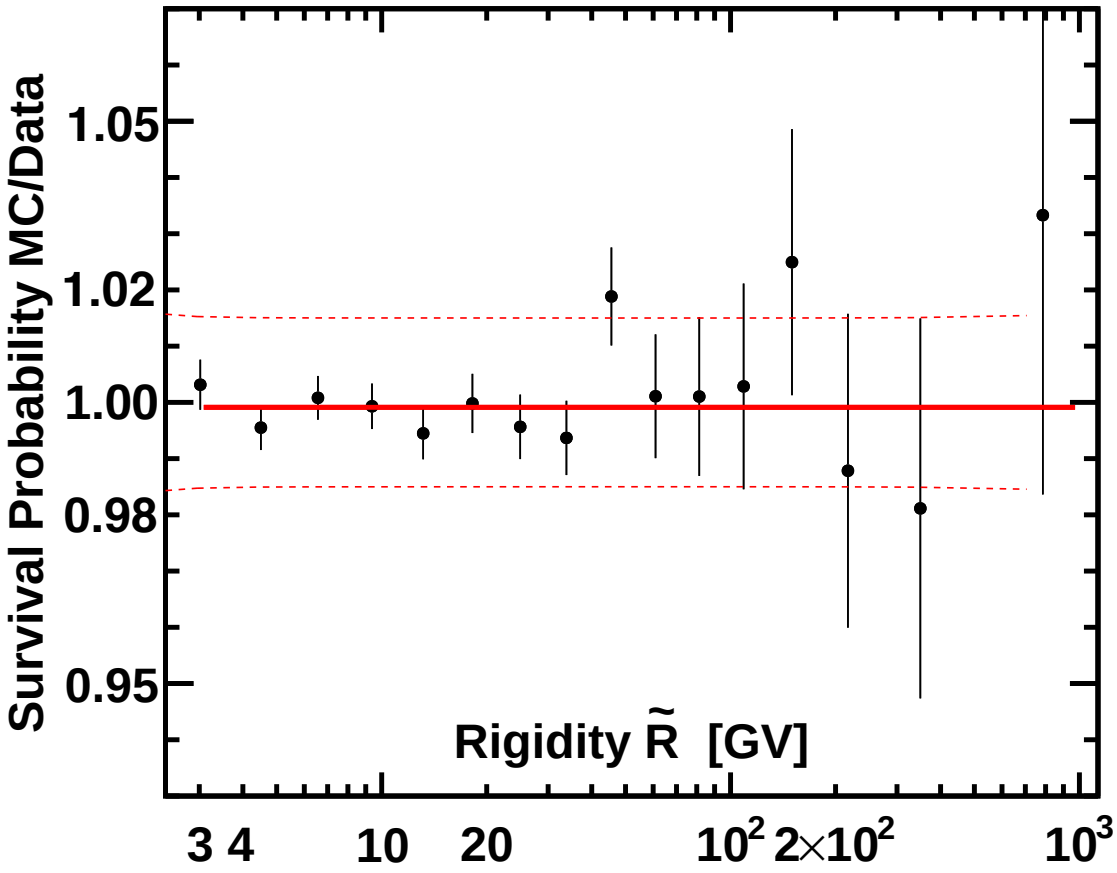

FIG. SM 5. The MC/data ratio of the nitrogen survival probabilities between $L8$ and $L9$. The solid line shows the constant fit to the data and the dashed lines indicate the systematic error range (68% CL).

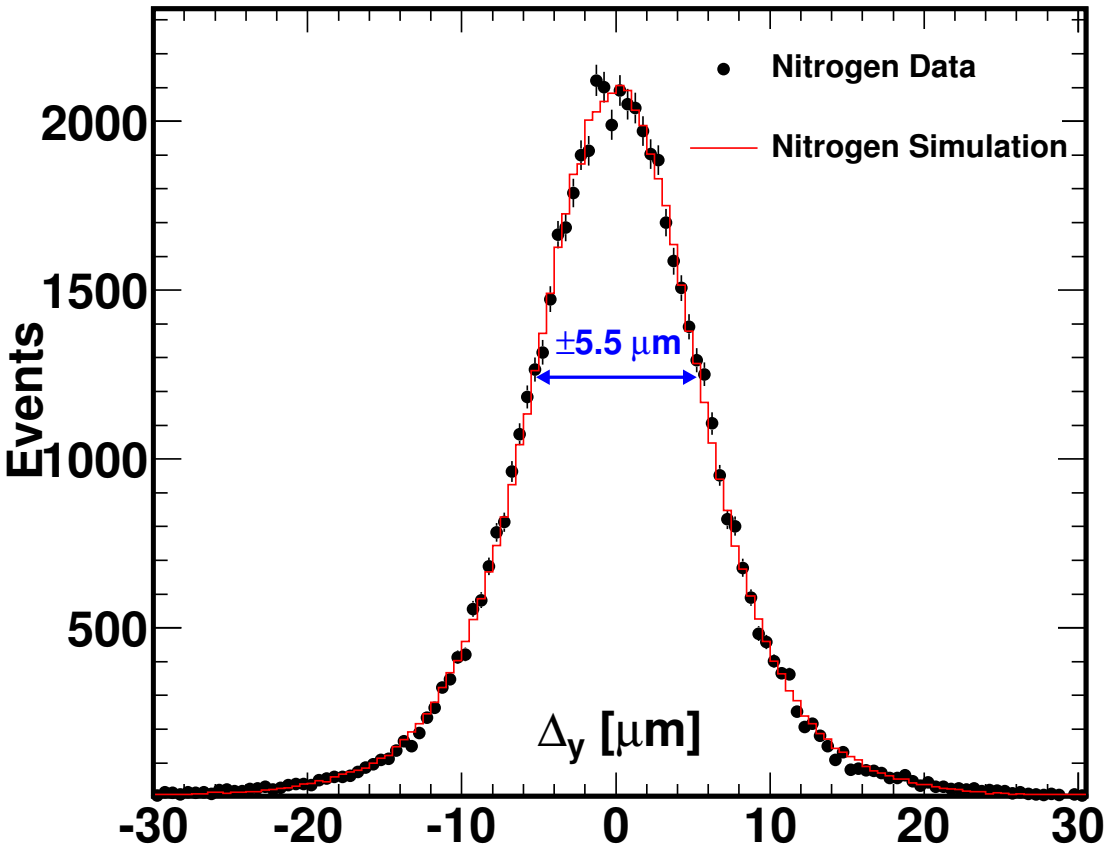

FIG. SM 6. Comparison of the differences of the coordinates measured in $L3$ or $L5$ to those obtained from the track fit using the measurements from $L1$, $L2$, $L4$, $L6$, $L7$, and $L8$ between data and simulation in the rigidity range $R > 50$ GV for nitrogen samples. The observed bending coordinate resolution is 5.5 μm.

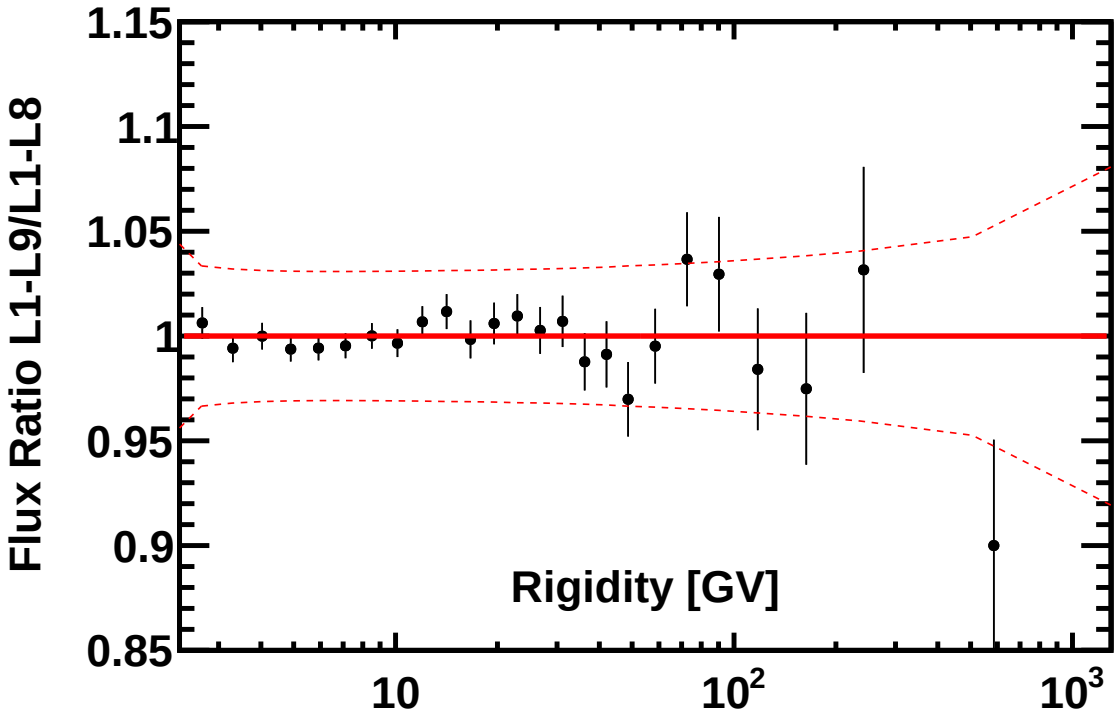

FIG. SM 7. The ratio of the nitrogen flux measured with events passing through $L1$ to $L9$ to the flux measured with events passing through $L1$ to $L8$. Error bars correspond to the statistical errors. The dashed red lines show the systematic errors. The solid red line is placed at unity to guide the eye.

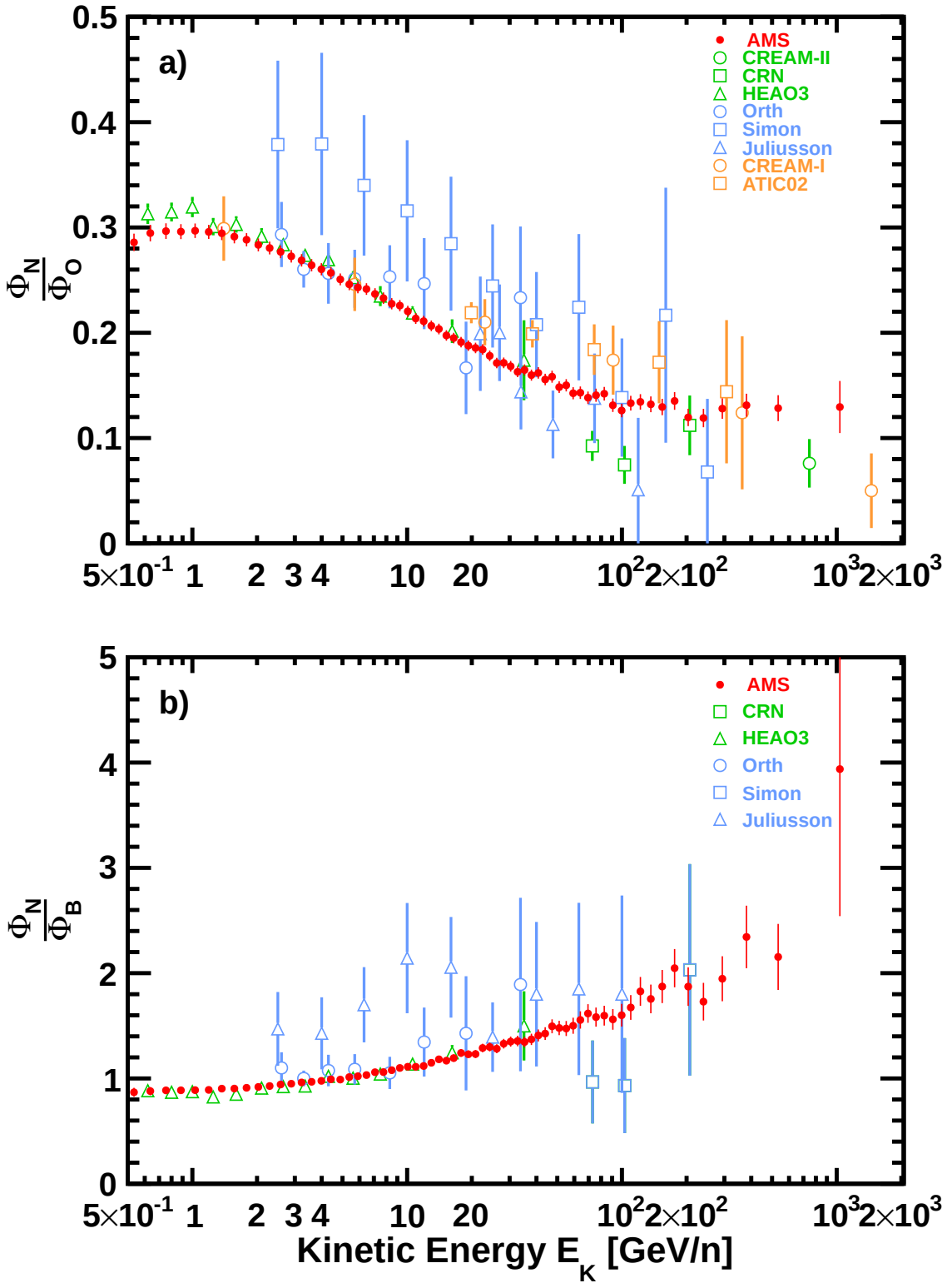

FIG. SM 8. (a) The AMS $\frac{\Phi_N}{\Phi_O}$ ratio as a function of kinetic energy per nucleon E_K together with earlier measurements. (b) The AMS $\frac{\Phi_N}{\Phi_B}$ ratio as a function of kinetic energy per nucleon E_K together with earlier measurements.

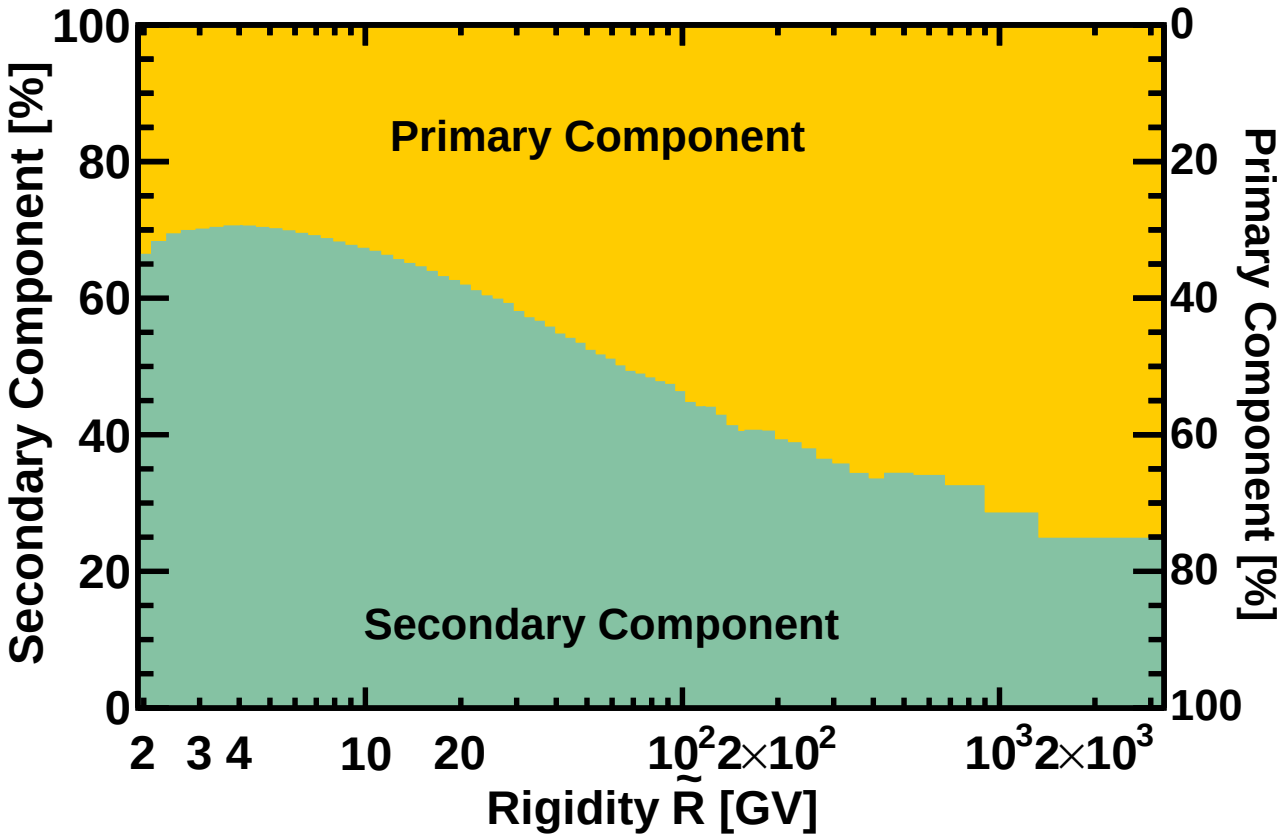

FIG. SM 9. The contributions of primary (yellow, right axis) and secondary (green, left axis) components of the nitrogen flux as functions of rigidity. As seen, the contribution of secondary component in the nitrogen flux drops from 70% at a few GV to below 30% above 1 TV.